

# Point Set Registration through Minimization of the $L_2$ Distance between 3D-NDT Models

Todor Stoyanov, Martin Magnusson and Achim J. Lilienthal  
Center of Applied Autonomous Sensor Systems (AASS), Örebro University, Sweden

**Abstract**—Point set registration — the task of finding the best fitting alignment between two sets of point samples, is an important problem in mobile robotics. This article proposes a novel registration algorithm, based on the distance between Three-Dimensional Normal Distributions Transforms. 3D-NDT models — a sub-class of Gaussian Mixture Models with uniformly weighted, largely disjoint components, can be quickly computed from range point data. The proposed algorithm constructs 3D-NDT representations of the input point sets and then formulates an objective function based on the  $L_2$  distance between the considered models. Analytic first and second order derivatives of the objective function are computed and used in a standard Newton method optimization scheme, to obtain the best-fitting transformation. The proposed algorithm is evaluated and shown to be more accurate and faster, compared to a state of the art implementation of the Iterative Closest Point and 3D-NDT Point-to-Distribution algorithms.

## I. INTRODUCTION

Point set registration is a task of fundamental importance in many application areas — computer vision, computational geometry, image processing to name but a few. In robotics, registration is often needed when fusing range sensor observations acquired at different physical locations. Fast and reliable registration is necessary for online Simultaneous Localization and Mapping, navigation, object modeling and other tasks.

Rigid body registration algorithms can generally be partitioned in two sets — global and local, depending on the search method they employ. Local methods rely on the assumption that a sufficiently good initial guess for the relative position and orientation between the two point sets is available. Global methods, on the other hand, are usually based on local geometrical features that can be uniquely matched, without any assumptions on the initial state (see for example Rusu et al. [1], Pathak et al. [2].) One of the most influential algorithms for point set registration in three dimensions — the Iterative Closest Point (ICP) method [3] belongs to the local optimization methods class. ICP is simple to implement and often converges to the correct solution. Many modifications of ICP have been proposed (Nüchter et al. [4], Granger et al. [5], Segal et al. [6] for example) in order to improve the algorithm's robustness to outliers, its convergence speed and to reduce the bias towards maximizing scan overlap.

A different local 3D point set registration method is based on the Three-Dimensional Normal Distributions Transform (3D-NDT). This article builds upon previous work on 3D-NDT registration by Magnusson [7]. A novel algorithm that minimizes the  $L_2$  distance between 3D-NDT models

is proposed and used to perform point set registration. An evaluation and comparison with a previous 3D-NDT approach and two reference state of the art registration algorithms is performed, demonstrating better accuracy and speed performance of the proposed method.

This article proceeds with a short introduction of the 3D-NDT and prior work on 3D-NDT registration. Section III then describes the motivation and derivation of the proposed registration algorithm. Finally, the performance of the approach is evaluated and discussed in Section IV.

## II. 3D-NDT REGISTRATION

### A. Point Set Modeling with the 3D-NDT

The Normal Distributions Transform was originally developed in the context of 2D laser scan registration [8]. The central idea is to represent the observed range points as a set of Gaussian probability distributions. In order to better account for outliers in the data, a mixture of a Gaussian distribution and a uniform distribution may also be used [9]. NDT has later been extended to three dimensions [10] and applied to the domains of 3D scan registration [11] and loop detection [7], as well as change detection [12] and path planning [13]. One of the key advantages of the 3D-NDT is the fact that it forms a piecewise smooth spatial representation, resulting in the existence of analytic derivatives. Consequently, standard optimization methods can be employed to produce state-of-the-art registration of 3D point clouds using the 3D-NDT representation [11]. After registration, a complete 3D-NDT map, which can be used for further tasks [14], can be created from the individual scans using a global network-optimization scheme.

Assuming that a set of  $n$  point samples  $\mathcal{P} = \{p_i = (x_i, y_i, z_i)\}$  with  $i = 1, \dots, n$  has been drawn from a Gaussian distribution  $\mathcal{N}(\mu, \Sigma)$ , the maximum likelihood estimates of the covariance and mean can be obtained from the observations:

$$\mu = \frac{1}{n} \sum_{i=1}^{i=n} p_i \quad (1)$$

$$M = [p_1 - \mu \dots p_n - \mu] \quad (2)$$

$$\Sigma = \frac{1}{n-1} M M^T \quad (3)$$

The 3D-NDT partitions space into a set of disjoint voxels and fits a Gaussian distribution to the points in each cell. In order to obtain a well-fitting estimate, it is important

最开始是2D的模型

这里说3D-NDT的关键优势就是它使用平滑的空间代表, 最终导致导数的出现, 这样对标准的优化方法非常有利

也就是每个voxel没有相交的点

to choose a discretisation strategy that would permit for each distribution to be well supported by the observations in  $\mathcal{P}$ . The most typical implementation of 3D-NDT utilizes a regular grid, though the use of an octree data structure of irregular cell size is also possible [7]. As shown previously, the spatial indexing used has an effect on the representation accuracy of the 3D-NDT [15], as well as on the speed and accuracy of the registration algorithms that utilize it [7].

### B. Point-to-Distribution Registration

Given a *fixed* reference point set  $\mathcal{F}$  and a *moving* point set  $\mathcal{M}$  from a nearby physical location, the registration task estimates the parameters  $\Theta$  of a transformation function  $T$ , such that  $T(\mathcal{M}, \Theta)$  is correctly aligned with respect to  $\mathcal{F}$ . Previous work by Magnusson [7] proposed to first construct the 3D-NDT of the fixed set  $M_{NDT}(\mathcal{F})$ . The likelihood that a point  $\mathbf{x} \in \mathcal{M}$  is generated from  $M_{NDT}(\mathcal{F})$  is

$$p(\mathbf{x}|M_{NDT}(\mathcal{F})) = \sum_{i=1}^{n_{\mathcal{F}}} w_i \mathcal{N}(\mathbf{x}|\boldsymbol{\mu}_i, \Sigma_i), \quad (4)$$

where  $n_{\mathcal{F}}$  is the number of Gaussian components of the 3D-NDT model of the point scan  $\mathcal{F}$  and  $w_i$  are normalization weights. The 3D-NDT registration algorithm minimizes an approximation of the negative log likelihood function of  $p(T(\mathcal{M}, \Theta)|M_{NDT}(\mathcal{F}))$ , over the space of transformation parameters  $\Theta$ . Thus, the registration problem is posed as minimizing the objective function:

$$f_{p2d}(\mathcal{M}, \mathcal{F}, \Theta) = -d_1 \sum_{j=1}^{|\mathcal{M}|} \exp \frac{-d_2}{2} (\mathbf{t}_j - \boldsymbol{\mu}_{\mathbf{m}})^T \Sigma_{\mathbf{m}}^{-1} (\mathbf{t}_j - \boldsymbol{\mu}_{\mathbf{m}}), \quad (5)$$

where  $d_1$  and  $d_2$  are positive regularizing factors,  $j$  iterates over all points  $\mathbf{m}_j \in \mathcal{M}$ ,  $\mathbf{t}_j = T(\mathbf{m}_j, \Theta)$  denotes a transformed point in the moving scan and  $(\boldsymbol{\mu}_{\mathbf{m}}, \Sigma_{\mathbf{m}})$  are the parameters of the normal distribution in  $M_{NDT}(\mathcal{F})$ , closest to the transformed current point  $\mathbf{t}_j$ . The objective function  $f_{p2d}$  is doubly differentiable with analytic expressions for the gradient and hessian. This approach of registering points to 3D Gaussian Distributions produces good registration results, using standard non-linear optimization methods.

## III. DISTRIBUTION-TO-DISTRIBUTION 3D-NDT REGISTRATION

### A. Background

This section presents a different perspective on the point set registration problem. Instead of maximizing the likelihood of a discrete set of points  $\mathcal{M}$  as in the previous subsection, the registration problem is interpreted as minimizing the distance between two 3D-NDT models  $M_{NDT}(\mathcal{F})$  and  $M_{NDT}(\mathcal{M})$ . As mentioned earlier, a 3D-NDT model can be viewed as a probability density function, signifying the likelihood of observing a point in space, belonging to an object surface (as in (4)). This formulation is equivalent to a Gaussian Mixture Model (GMM) with uniform weights and largely disjoint components. Several possible distance

metrics between probability distributions can be used to formulate the Distribution-to-Distribution objective function.

This section reviews some of the related work in GMM registration and motivates the choice of a distance metric.

Several statistical metrics are commonly used to compute the distance between probability distributions. The Kullback Leibler Divergence  $KL(R||S)$  measures the expected additional information needed to explain the information carried by the random variable  $S$ , using the random variable  $R$ . The symmetric KL Divergence  $SKL(R||S) = KL(R||S) + KL(S||R)$  is commonly used to compare two probability distributions in an unbiased way. Although approximations of the KL Divergence for GMMs exist [16][17], most are based on sampling and cannot be used for analytical purposes. Hershey and Olsen [16] propose three different closed-form variational bounds to the KL-Divergence between GMMs. An approach based on their approximations was implemented, but resulted in unsatisfactory performance, due to the too general nature of the proposed bounds. Other distance metrics include the Bhattacharyya and closely related Hellinger Distance, both of which do not have analytic solutions for GMMs, and were therefore not be considered.

Another approach is to use mutual information  $\mathcal{I}(M_{NDT}(\mathcal{M}), M_{NDT}(\mathcal{F}))$  as a distance metric. Wells et al. [18] propose an algorithm that maximizes the mutual information between kernel density estimates of MRI and CT images, by reformulating mutual information as a joint entropy. While the entropy of a single Gaussian component has a closed form solution, no analytic expression can be obtained for a GMM. The most popular approach, also applied by Wells et al. [18] is to compute the entropy explicitly using Monte Carlo sampling. This, however, is slow and forbids the computation of analytical derivatives. A recent work by Huber et al. derives several closed-form approximations of GMM entropy, based on Taylor series expansions [19]. An approach based on these results is feasible, but would encounter the serious difficulty of estimating the joint density of the two 3D-NDTs.

### B. Registration Based on $L_2$ Distance

A different approach to GMM registration is to minimize the  $L_2$  norm between the probability density functions, over all possible inputs. A point set registration algorithm that utilizes this strategy was proposed and formalized by Jian et al [20], building on previous related work on kernel correlation by Tsin et al. [21]. The work by Jian et al. proposes to compute and register a fixed-width spherical Gaussian kernel density estimate of each point cloud. The rest of this section extends their approach to the more general, variable kernel size 3D-NDT representation.

The  $L_2$  distance between two 3D-NDTs (or GMMs) is defined as:

$$D_{L_2}(\mathcal{M}, \mathcal{F}, \Theta) = \int \left( p(\mathbf{x}|M_{NDT}(\mathcal{F})) - p(\mathbf{x}|T(M_{NDT}(\mathcal{M}), \Theta)) \right)^2 d\mathbf{x} \quad (6)$$

or equivalently,

$$D_{L_2}(\mathcal{M}, \mathcal{F}, \Theta) = \int p(\mathbf{x}|M_{NDT}(\mathcal{F}))^2 d\mathbf{x} + \int p(\mathbf{x}|T(M_{NDT}(\mathcal{M}), \Theta))^2 d\mathbf{x} - 2 \int p(\mathbf{x}|M_{NDT}(\mathcal{F}))p(\mathbf{x}|T(M_{NDT}(\mathcal{M}), \Theta))d\mathbf{x}, \quad (7)$$

where  $T(X, \Theta)$  is a parametrized transformation function, as in the previous subsection. It is useful to interpret this expression, using Renyi's Quadratic Entropy (RQE)  $H_{rqe}$ , defined as:

$$H_{rqe}(P(\mathbf{x})) = - \int P^2(\mathbf{x})d\mathbf{x}. \quad (8)$$

Evidently, Equation 7 can be interpreted as the sum of the RQEs of the model and transformed scan, plus an additional term that relates to the mixing of the two GMMs. Both entropies are invariant over rigid transformations and can be disregarded for the objective function. As Jian et al. [20] note, the third term can be simplified using the following identity:

$$\int \mathcal{N}(\mathbf{x}|\boldsymbol{\mu}_i, \Sigma_i)\mathcal{N}(\mathbf{x}|\boldsymbol{\mu}_j, \Sigma_j)d\mathbf{x} = \mathcal{N}(0|\boldsymbol{\mu}_i - \boldsymbol{\mu}_j, \Sigma_i + \Sigma_j) \quad (9)$$

Thus, a final expression for the  $L_2$  distance to be minimized is obtained:

$$D_{L_2}(\mathcal{M}, \mathcal{F}, \Theta) \sim \sum_{i=1}^{n_{\mathcal{M}}} \sum_{j=i}^{n_{\mathcal{F}}} \mathcal{N}(0|T(\boldsymbol{\mu}_i, \Theta) - \boldsymbol{\mu}_j, T(\Sigma_i, \Theta) + \Sigma_j), \quad (10)$$

with  $n_{\mathcal{M}}$  and  $n_{\mathcal{F}}$  being the number of Gaussian components in  $M_{NDT}(\mathcal{M})$  and  $M_{NDT}(\mathcal{F})$  respectively.

The transformation function  $T(\cdot, \Theta)$  can be parametrized using different rotation representations. For this work, an Euler angle parametrization has been used to define a rotation matrix  $R$ . The parameters of the transformation are accumulated in a vector  $\mathbf{p} = (t_x, t_y, t_z, r_x, r_y, r_z)$ , with translation vector  $\mathbf{t} = (t_x, t_y, t_z)$ , and  $x - y - z$  Euler angles  $r_x, r_y, r_z$ . The objective function of the Distribution-to-Distribution registration algorithm is defined as:

$$f_{d2d}(\mathbf{p}) = \sum_{i=1}^{n_{\mathcal{M}}} \sum_{j=i}^{n_{\mathcal{F}}} -d_1 \exp\left(-\frac{d_2}{2} \boldsymbol{\mu}_{ij}^T (R^T \Sigma_i R + \Sigma_j)^{-1} \boldsymbol{\mu}_{ij}\right), \quad (11)$$

where  $\boldsymbol{\mu}_{ij}(\mathbf{p})$  is the transformed mean vector distance:

$$\boldsymbol{\mu}_{ij}(\mathbf{p}) = R\boldsymbol{\mu}_i + \mathbf{t} - \boldsymbol{\mu}_j. \quad (12)$$

The gradient vector of the Distribution-to-Distribution NDT registration function can then be derived, component-wise as:

$$\frac{\partial}{\partial p_a} f_{d2d}(\mathbf{p}) = \frac{d_1 d_2}{2} (\boldsymbol{\mu}_{ij}^T B \mathbf{j}_a - \boldsymbol{\mu}_{ij}^T B Z_a B \boldsymbol{\mu}_{ij}) \exp\left(-\frac{d_2 \boldsymbol{\mu}_{ij}^T B \boldsymbol{\mu}_{ij}}{2}\right), \quad (13)$$

with  $p_a$  being a component of the pose vector  $\mathbf{p}$  and the following component expressions

$$B = (R^T \Sigma_i R + \Sigma_j)^{-1} \quad (14)$$

$$\mathbf{j}_a = \frac{\partial}{\partial p_a} (R\boldsymbol{\mu}_i + \mathbf{t} - \boldsymbol{\mu}_j) \quad (15)$$

$$Z_a = \frac{\partial}{\partial p_a} (R^T \Sigma_i R) \quad (16)$$

Similarly, the Hessian matrix is:

$$\begin{aligned} \frac{\partial^2}{\partial p_a \partial p_b} f_{d2d}(\mathbf{p}) = & d_1 d_2 \left( \mathbf{j}_a^T B \mathbf{j}_b - 2 \boldsymbol{\mu}_{ij}^T B Z_a B \mathbf{j}_b + \right. \\ & \boldsymbol{\mu}_{ij}^T B H_{ab} - \boldsymbol{\mu}_{ij}^T B Z_a B Z_b B \boldsymbol{\mu}_{ij} - \\ & \left. \frac{1}{2} \boldsymbol{\mu}_{ij} B Z_{ab} B \boldsymbol{\mu}_{ij} - \frac{d_2}{4} \mathbf{q}^T \mathbf{q} \right) \\ & \exp\left(-\frac{d_2 \boldsymbol{\mu}_{ij}^T B \boldsymbol{\mu}_{ij}}{2}\right), \end{aligned} \quad (17)$$

where

$$H_{ab} = \frac{\partial^2}{\partial p_a \partial p_b} (R\boldsymbol{\mu}_i + \mathbf{t} - \boldsymbol{\mu}_j) \quad (18)$$

$$Z_{ab} = \frac{\partial^2}{\partial p_a \partial p_b} (R^T \Sigma_i R) \quad (19)$$

$$\mathbf{q} = \boldsymbol{\mu}_{ij}^T B \mathbf{j}_a - \boldsymbol{\mu}_{ij}^T B Z_a B \boldsymbol{\mu}_{ij}. \quad (20)$$

The first and second derivatives of the transformation function  $T(\mathbf{p})$  are easily calculated for each component of the pose vector  $\mathbf{p}$  and stored in the expressions  $\mathbf{j}_a, Z_a, H_{ab}, Z_{ab}$ . Due to space limitations, the precise derivative expressions in terms of  $(t_x, t_y, t_z, r_x, r_y, r_z)$  have been omitted. The so defined objective and derivatives are used as inputs to a Newton method optimization routine with a More-Thuente line search for step control. To speed-up computation, the current version of the registration algorithm only considers the pairwise closest components from both 3D-NDTs. As the component distributions of each 3D-NDT are largely disjoint, this presents for a reasonable approximation of the objective function. Thus, the objective (11) and its derivatives are evaluated only at each pair of closest components from the models  $M_{NDT}(\mathcal{M})$  and  $M_{NDT}(T(\mathcal{S}, \Theta))$ . The performance of the proposed algorithm is evaluated in the next section.

### C. Relation to Iterative Closest Point Methods

It may be worth noting the relationship of the algorithm proposed in the previous sections to prior work on ICP registration. Two notable similar works were proposed by Segal et al. [6] and Jian and Vemuri [20]. Both of these works present generalizations of the ICP algorithm through the use of a modified distance metric function. In this respect, the objective functions presented in these works are similar to the objective proposed in (11). Jian and Vemuri propose the use of a covariance-norm based distance function. The key difference to our approach lies in the construction of the covariance matrix  $\Sigma$ , which Jian and Vemuri assume to be spherical and parametrized only by a variance  $\sigma$  along the main diagonal. Moreover,  $\sigma$  is a stationary parameter — it



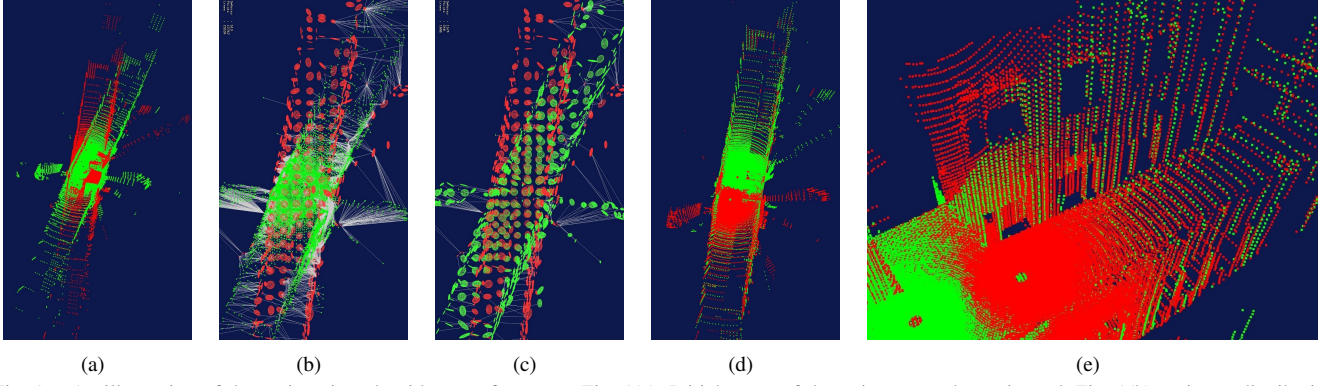


Fig. 1. An illustration of the registration algorithms performance. Fig. 1(a): Initial poses of the point sets to be registered. Fig. 1(b): point-to-distribution registration first iteration with correspondences drawn as lines. Fig. 1(c): distribution-to-distribution first iteration, correspondences drawn as lines. Fig. 1(d): Final pose from distribution-to-distribution registration. Fig 1(e): a detail from the registered scan, different point clouds shown in red and green.

does not change for any location in  $\mathbb{R}^3$ . In the algorithm presented in this chapter, the covariance  $\Sigma$  is non-stationary and is estimated, based on the local structure of the registered point clouds.

The method proposed by Segal et al. [6] — Generalized-ICP formulates an objective function based on the error between points, that are assumed to be drawn from independent Gaussian distributions. Thus, the objective function is similar to (11). There are, however, several important differences between 3D-NDT-D2D and Generalized-ICP. First of all, the way the covariance matrix is estimated differs — the application of Generalized-ICP discussed by Segal et al. assumes locally planar patches around each point, then calculates the normal direction to the local surface and uses it to bias the orientation of the covariance matrix. Second, the way that the optimal transformation parameters  $T(\cdot, \Theta)$  are estimated is different — namely Generalized ICP relies on a conjugate gradient descent with numerical evaluation of derivatives, while 3D-NDT-D2D uses a Newton's method with analytical derivative expressions. Last but not least, 3D-NDT-D2D operates only on the estimated Gaussian components of the 3D-NDT models  $M_{NDT}(\mathcal{F})$  and  $M_{NDT}(\mathcal{M})$ , opposed to the full sets of point samples  $\mathcal{F}$  and  $\mathcal{M}$ , thus allowing for a significantly reduced number of corresponding components considered in the evaluation of the objective function. The reduction in components, due to the compactness of the 3D-NDT representation, leads to lower runtimes, discussed in details in the results in the next section.

#### IV. EVALUATION

This section presents a preliminary evaluation of the proposed distribution-to-distribution 3D-NDT registration algorithm. Both the proposed algorithm and the original point-to-distribution method were implemented in the same framework and evaluated on sample inputs. After discussing the reference implementations, this section proceeds with results and analysis of the performance.

The point-to-distribution 3D-NDT registration algorithm was implemented and integrated as a package for the Robot Operating System (ROS) [22]. The version used for comparison in this work evaluates the likelihood of each point in  $T(\mathcal{S}, \Theta)$  with respect to only the closest Gaussian component

Scan Pair	Features of the Scanned Environment
1	cross-roads corridor, very few features
2	large room, a lot of clutter from furniture
3	large room and corridor, clutter
4	corridor and hallway, no clutter
5	corridor and stair case, no clutter, moderate features

TABLE I

FEATURES OF THE TEST SET SCAN PAIRS

in  $N(\mathcal{M})$ . The metaparameters  $d_1$  and  $d_2$  are computed in the same way as previous work by Magnusson [7]. All tests were performed with iterative optimization at 3D-NDT grid sizes of 4, 2, 1 and 0.5 meters.

The distribution-to-distribution registration algorithm was implemented in the same framework. For each component of  $N(T(\mathcal{S}, \Theta))$ , only the closest distribution in  $N(\mathcal{M})$  was used in evaluating Equation 11. As the components of the 3D-NDT are largely non-overlapping, this approximation should not result in significant changes of the behavior of the score function. The values of meta-parameters were determined empirically and set to  $d_1 = 1$  and  $d_2 = 0.05$  respectively. The significance of these values is further discussed at the end of this section. Tests were again performed with iterative optimization at 3D-NDT grid sizes of 4, 2, 1 and 0.5 meters. Finally, all source code developed is available at <http://code.google.com/p/oru-ros-pkg/>.

Several tests were performed in order to evaluate the performance of the presented registration algorithm. Point clouds from the AASS-loop data set (available at <http://kos.informatik.uni-osnabrueck.de/3Dscans>) were used. The point sets were collected with an actuated SICK LMS-200 laser scanner, mounted on a mobile robot. Five different scan pairs were selected, manually registered (by aligning the point sets using a combination of 3D-NDT-D2D and hand-picked transformations) and henceforth used as ground truth reference for the tests. An example scan pair (scan pair 5 in subsequent discussions) and the output of the first iteration of the registration algorithms are shown in Figure 1, while the properties of the chosen benchmark point scans are described in Table I.

Using the manually registered point set pairs, test scenarios for the registration algorithms were generated. One of the point sets in the pair was transformed away from the ground

这里给出了  
Ground truth的  
获取方法

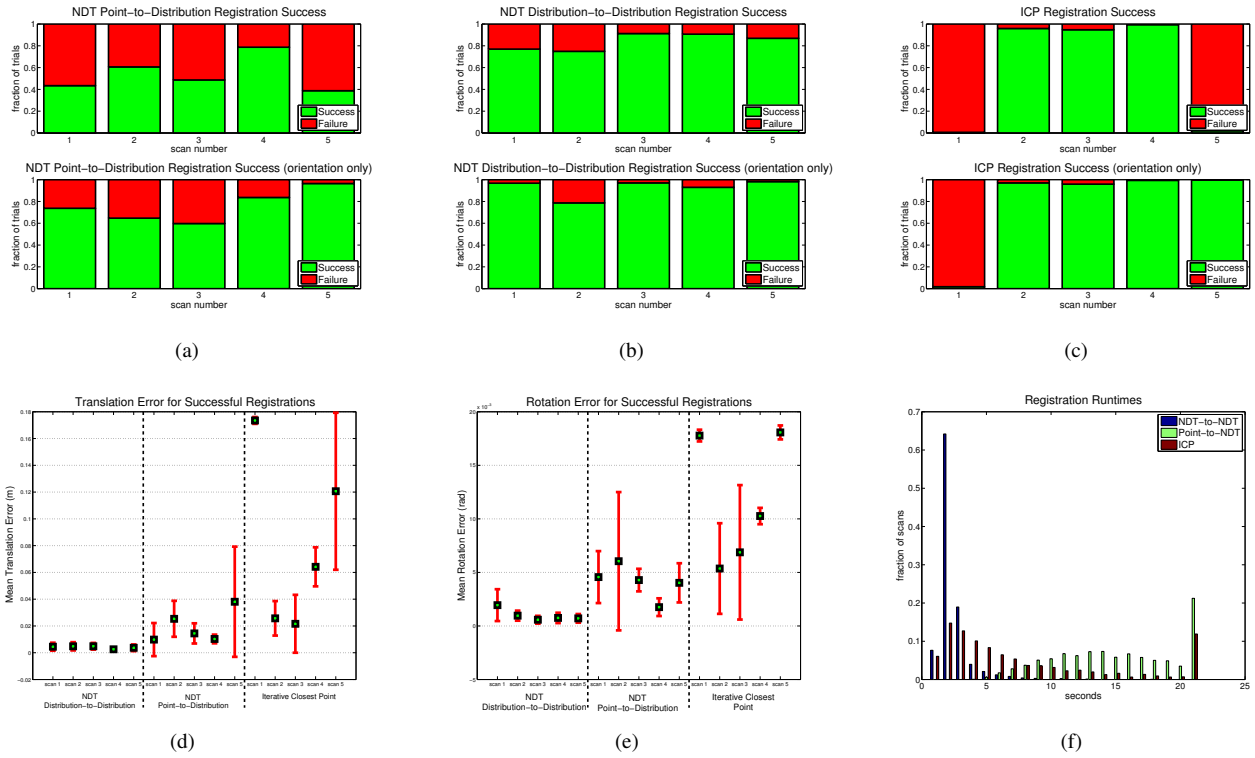


Fig. 2. Summary of results of the evaluated registration methods, over all five scan pairs. Fig 2(a): point-to-distribution 3D-NDT success rates with (top) and without (bottom) considering translation errors. Fig 2(b): distribution-to-distribution success rates. Fig 2(c): ICP success rates. Mean translation 2(d) and rotation 2(e) error for the successfully registered scans. Fig. 2(f): run times distribution for the three algorithms.

truth position and then used as an input to the evaluated registration algorithm. For each of the five test pairs, offsets of between  $-1.5$  and  $1.5$  meters in steps of  $0.5$  meters (along the  $x$  and  $y$  axes) were introduced. Additionally, the scans were rotated around the  $z$  axis by an angle varying from  $-30$  to  $30$  degrees (in steps of  $10^\circ$ ). Thus, a total of 343 test transformations (combinations of seven distinct points along  $t_x$ ,  $t_y$  and  $r_z$ ) were generated and applied to the scan point set  $\mathcal{S}$ . Registration was judged to be successful if the output transformation brought the scan  $\mathcal{S}$  within  $0.2$  meters and  $0.05$  radians from its ground truth position.

Previous work by Magnusson et al. [11] compared the performance of the point to distribution 3D-NDT registration algorithm to that of a highly-optimized version of the ICP algorithm, developed by Nüchter et al. [4]. Results showed that 3D-NDT performed better overall, with a high robustness to outliers, occlusions and low scan overlap. In order to compare the newly implemented registration algorithms, a comparison to two baseline registration algorithms was also performed. The standard ICP package from ROS was used as one of the reference implementations, while the Fast Point Feature Histogram (FPFH) with Sample Consensus Initial Alignment (SAC-IA) provided a second point of comparison. As described by Rusu et al. [1], FPFH with SAC-IA is a global registration method — thus, the initial alignment of the scans does not matter. Results of using only this initial alignment step are reported, but it should be noted that a local method (ICP in this case) was used to produce a refined final result as well.

The performance of the discussed registration algorithms over all five test sets is summarized in Figure 2 and Table II. Overall, the newly proposed distribution-to-distribution 3D-NDT registration algorithm slightly outperforms the point-to-distribution implementation tested in this work. The performance of the base-line ICP algorithm is very good on scan pairs 2,3 and 4 and extremely poor on scan 1 and 5. It is worth noting that the problematic scan pairs represent a typical failure case for ICP — a corridor environment with largely overlapping, feature poor scans. The second reference approach — SAC-IA with FPFH features did not deliver promising results. The initial alignments provided by the approach were very poor on scan pairs 1 and 5, and borderline on the remaining test pairs. After ICP refinement, however, the results for sets 2, 3 and 4 improved significantly. Figure 2(d) and 2(e) summarize the mean translational and rotational errors over all successfully registered point set pairs. The distribution-to-distribution algorithm proposed exhibits a stable performance over all tests, with a small variance in the error scores. Note that for the point-to-distribution and especially for the ICP algorithm, the results for scan pairs 1 and 5 were obtained from a much smaller sample of successful registrations.

Figure 2(f) also summarizes the run times of the evaluated registration methods. All tests were performed on a 3GHz Intel Core2 Duo processor with 3.2GB of RAM. On average, the input point sets contained 110k points each, resulting in between 600 and 1300 Normal distributions at the finest grid size of  $0.5m$ . Constructing the 3D-NDT models took

	Scan1	Scan2	Scan3	Scan4	Scan5
SAC-IA+FPFH:					
Translation Error (m)	3.51	2.75	1.09	0.49	2.01
Rotation Error (rad)	3.21	0.57	0.63	0.47	3.13
Runtime (s)	50.2	53.3	52.0	49.5	65.8
SAC-IA+FPFH+ICP:					
Translation Error (m)	1.41	0.28	0.21	0.27	2.12
Rotation Error (rad)	3.1	0.06	0.02	0.02	3.18
Runtime (s)	128.7	130.0	56.3	80.3	68.9

TABLE II  
RESULTS FOR FEATURE-BASED REGISTRATION

on average 0.2 seconds per scan and is included in the reported cumulative runtimes. As expected, the distribution-to-distribution method resulted in much faster computation times, averaging 1.9 seconds over all tested scans. The original point-to-distribution method averaged 16.5 seconds per scan, using a subsampling ratio of roughly 20% for the moving scan  $\mathcal{S}$ . The ICP algorithm averaged 10.1 seconds, with a 0.1 meter grid subsampling, while the FPFH alignment took well above 50 seconds. As the run times for the point-to-distribution 3D-NDT are slower than the ones reported for previous implementations, it is possible that a faster numerical optimization implementation would produce much better results for both NDT based algorithms.

Finally, it is important to discuss the influence of the regularization parameters  $d_1$  and  $d_2$  on the convergence properties of the proposed registration algorithm. While these parameters do not affect the location of the global minimum, they change the shape of the objective and the depth of the local minima. Modifying  $d_1$  results in scaling of the entire objective and consequently can influence the numerical stability of the algorithm. The parameter  $d_2$  controls the spread or area of influence of each local minimum. Smaller values of  $d_2$  are desirable, as they result in smoother objectives, but can also lead to less pronounced global minima. Finding optimal parameter values is an important problem and will be further addressed in the future.

## V. DISCUSSION

This article presented a novel algorithm for point set registration, using the Three-Dimensional Normal Distributions Transform. An objective function, based on the  $L_2$  distance between Gaussian Mixture Models was devised and used to register 3D-NDT models. Analytic first and second order derivatives of the objective function were computed and used in a Newton method optimization scheme. The proposed algorithm was evaluated and compared against an implementation of the point-to-distribution 3D-NDT registration method. The accuracy of the proposed algorithm was found to be comparable and in some cases better than that of the previous approach, standard ICP and FPFH global alignment, while the registration speed was significantly increased. Further improvements of the accuracy and speed of the proposed algorithm will be pursued as future work. Major directions to be considered are the tuning of parameters (focusing on the regularization factors), more accurate evaluation of the objective function and the exploration of faster converging optimization schemes.

## REFERENCES

- [1] R. B. Rusu, N. Blodow, and M. Beetz, "Fast Point Feature Histograms (FPFH) for 3D registration," in *IEEE Int. Conf. on Robotics and Automation, ICRA 2009*, pp. 3212–3217.
- [2] K. Pathak, A. Birk, N. Vaskevicius, and J. Poppinga, "Fast Registration Based on Noisy Planes With Unknown Correspondences for 3-D Mapping," *Robotics, IEEE Transactions on*, vol. 26, no. 3, pp. 424–441, June 2010.
- [3] P. Besl and N. McKay, "A Method for Registration of 3-D Shapes," *IEEE Transactions on Pattern Analysis and Machine Intelligence*, vol. 14, pp. 239–256, 1992.
- [4] A. Nüchter, K. Lingemann, J. Hertzberg, and H. Surmann, "6D SLAM—3D mapping outdoor environments," *Journal of Field Robotics*, vol. 24, no. 8-9, pp. 699–722, 2007.
- [5] S. Granger and X. Pennec, "Multi-scale EM-ICP: A Fast and Robust Approach for Surface Registration," in *Computer Vision — ECCV 2002, Lecture Notes in Computer Science*, 2006, pp. 69–73.
- [6] A. Segal, D. Haehnel, and S. Thrun, "Generalized-ICP," in *Proceedings of Robotics: Science and Systems*, Seattle, USA, June 2009.
- [7] M. Magnusson, "The Three-Dimensional Normal-Distributions Transform — an Efficient Representation for Registration, Surface Analysis, and Loop Detection," Ph.D. dissertation, Örebro University, Dec. 2009.
- [8] P. Biber and W. Straßer, "The Normal Distributions Transform: A new Approach to Laser Scan Matching," in *Proc. of IEEE/RSJ Int. Conf. on Intelligent Robots and Systems. IROS 2003*, 2003.
- [9] P. Biber, S. Fleck, and W. Straßer, "A Probabilistic Framework for Robust and Accurate Matching of Point Clouds," in *26th Pattern Recognition Symposium (DAGM 04)*, 2004.
- [10] M. Magnusson, T. Duckett, and A. J. Lilienthal, "3D scan registration for autonomous mining vehicles," *Journal of Field Robotics*, vol. 24, no. 10, pp. 803–827, Oct. 24 2007.
- [11] M. Magnusson, A. Nüchter, C. Lörken, A. J. Lilienthal, and J. Hertzberg, "Evaluation of 3D Registration Reliability and Speed - A Comparison of ICP and NDT," in *Proc. IEEE Int. Conf. on Robotics and Automation, ICRA 2009*, pp. 3907–3912.
- [12] H. Andreasson, M. Magnusson, and A. J. Lilienthal, "Has Something Changed Here? Autonomous Difference Detection for Security Patrol Robots," in *Proc. of IEEE/RSJ Int. Conf. on Intelligent Robots and Systems. IROS 2007*, 2007.
- [13] T. Stoyanov, M. Magnusson, H. Andreasson, and A. J. Lilienthal, "Path Planning in 3D Environments Using the Normal Distributions Transform," in *Proc. of IEEE/RSJ Int. Conf. on Intelligent Robots and Systems. IROS 2010*, Taipei, Taiwan, 2010.
- [14] M. Magnusson, H. Andreasson, A. Nüchter, and A. J. Lilienthal, "Automatic Appearance-Based Loop Detection from 3D Laser Data Using the Normal Distributions Transform," *Journal of Field Robotics*, vol. 26, no. 11–12, pp. 892–914, Nov. 2009.
- [15] T. Stoyanov, M. Magnusson, H. Almqvist, and A. J. Lilienthal, "On the Accuracy of the 3D Normal Distributions Transform as a Tool for Spatial Representation," in *Proc. of IEEE Int. Conf. on Robotics and Automation, ICRA 2011*.
- [16] J. Hershey and P. Olsen, "Approximating the Kullback Leibler Divergence Between Gaussian Mixture Models," in *IEEE Int. Conf. on Acoustics, Speech and Signal Processing, ICASSP 2007*, vol. 4, 2007.
- [17] J. Goldberger, S. Gordon, and H. Greenspan, "An Efficient Image Similarity Measure Based on Approximations of KL-Divergence between two Gaussian Mixtures," in *Int. Conf. on Computer Vision, ICCV 2003*, 2008, pp. 487–493.
- [18] W. Wells III, P. Viola, H. Atsumi, S. Nakajima, and R. Kikinis, "Multimodal volume registration by maximization of mutual information," *Medical image analysis*, vol. 1, no. 1, pp. 35–51, 1996.
- [19] M. Huber, T. Bailey, H. Durrant-Whyte, and U. Hanebeck, "On Entropy Approximation for Gaussian Mixture Random Vectors," in *Int. Conf. on Multisensor Fusion and Integration for Intelligent Systems, MFI 2008*, 2008, pp. 181–188.
- [20] B. Jian and B. Vemuri, "Robust Point Set Registration Using Gaussian Mixture Models," *IEEE Transactions on Pattern Analysis and Machine Intelligence*, 2010.
- [21] Y. Tsing and T. Kanade, "A Correlation-Based Approach to Robust Point Set Registration," in *Computer Vision-ECCV 2004*, ser. Lecture Notes in Computer Science. Springer, 2004, pp. 558–569.
- [22] M. Quigley, K. Conley, B. P. Gerkey, J. Faust, T. Foote, J. Leibs, R. Wheeler, and A. Y. Ng, "ROS: an open-source Robot Operating System," in *ICRA Workshop on Open Source Software*, 2009.